

Flame Spread Over Electrical Wires with Various Diameters under Applied AC Electric Fields

S. H. Park¹, S. J. Lim², J. Park¹, O.B. Kwon¹, O. Fujita³, S. H. Chung⁴

¹ Department of Mechanical Engineering, Pukyong National University, Busan, Korea

² Advanced Combustion Laboratory, Korea Institute of Energy Research, Daejeon Korea

³ Division of Mechanical & Space Engineering, Hokkaido University, Sapporo, Japan

⁴ King Abdullah University of Science and Technology (KAUST), Clean Combustion Research Center (CCRC), Thuwal, Saudi Arabia

1 Introduction

Space technologies have been developed in various areas such as satellite, space hotel, international space station and space food. Electrical wire fire in space can result in extensive damages and fatalities, e.g., the Apollo 1 and the Mir Space Station. In this sense, developing fire safety code is an essential requirement for space development. Flame spread over electrical wire can be influenced by several factors, such as material properties of the inner core and outer insulator, gravity level, ambient flow, and pressure [1-6]. Wire fire can be caused by unexpected electrical short and/or overheating of wire. Thus, it can be actually under influence of electric fields. Even if an electrical shortage disconnects an electrical circuit during the initial and propagation stages of a wire fire, a wire can still be under the influence of an electric field. This type of electrode configuration behaves like an open circuit when voltage is applied. In such a case, the charged particles generated through chemi-ionization and subsequent ion chemistry in the reaction zone of a spreading flame can be influenced by the electric field through the Lorentz force. However, studies on the effect of applied electric fields on flame spread over electrical wire has been limited to two papers [7, 8]. Here, we report the effect of insulator diameter in flame spread over electrical wire with applied electric fields.

2 Experimental facility

Figure 1 shows a schematic of experimental apparatus, which consists of an electrical wire, a wire holder, an AC power supply, and a video camera. Polyethylene-insulated electrical wires of 400 mm in length housed 0.5 mm diameter (D_C) NiCr core and were coated with insulators of 0.8, 1.1 and 1.5 mm in diameter (D_{OUT}). The wire was installed on a wire holder made of nonconductive acetal resin. One end of a wire was

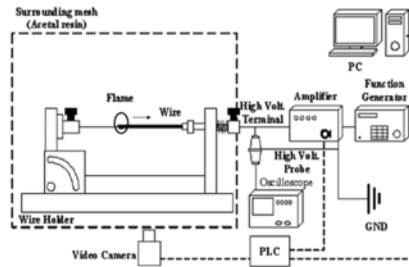


Figure 1 Schematic illustration of experimental setup

fixed to the wire holder and the other end of wire was connected to a spring in order to prevent bending of the wire due to thermal expansion during flame spread. The wire and wire holder were surrounded by acetal mesh to prevent outside disturbances. One end of the electrical wire was connected to high voltage terminal of the power supply and the other terminal was linked to building ground, resulting in one electrode configuration. The voltage (V_{AC}) and frequency (f_{AC}) applied to the wire were in range of 1 ~ 5 kV and 10 ~ 1000 Hz. The flame was ignited by an igniter which was placed on an air cylinder. In order to minimize the interaction between the ignition system and applied AC electric fields, igniter was removed away from the wire after ignition. The wire length was 247 mm, excluding the portion connected to the wire holder. Initial 70 mm from the one end of wire and final 10 mm were excluded due to ignition transition and interaction of the wire holder, respectively, leaving 167 mm of wire length available for flame spread. A video camera was triggered to capture spreading flame. Images were analyzed using a Matlab-based code.

3 Results and Discussion

3.1 Overall feature of spreading flame

Figure 2 shows representative flame images for several diameters with various applied f_{AC} at $V_{AC}=4$ kV. For $f_{AC} = 10$ Hz case, the size of spreading flame increased in increase of wire diameter due to growth of amount of insulator. In case of $f_{AC} = 30$ Hz, the spreading flame were tilted to bare wire compared with $f_{AC} = 10$ Hz. Also, the sizes of flames became smaller compared with the $f_{AC} = 10$ Hz. At $f_{AC}=200$ Hz, the size of flame became bigger compared with $f_{AC} = 30$ Hz and it was decreased again with an increased applied f_{AC} up to 1000 Hz. At $f_{AC}= 600$ (1000) Hz, the spreading flame was extinguished at $D_{OUT} = 0.8$ (1.1) mm. The results show that spreading flame does not extinguish at all frequencies and voltages in range of the current electric fields for $D_{OUT} = 1.5$ mm but extinguish at high frequencies and voltages for $D_{OUT} = 0.8$ and 1.1 mm. Figure 3 shows temporal positions of flame front X with time at several diameters for $V_{AC} = 4$ kV and $f_{AC} = 10$ Hz (a) and at various frequencies for (b) $D_{OUT} = 0.8$, (c) 1.1, (d) 1.5 mm. The position of flame front was identified as the flame front in contact with the electrical wire. In figure 3(a), the flame position varies almost linearly during flame spread. Thus, flame spread rate (FSR), $S_W = \Delta X / \Delta t$, was defined reasonably as the overall rate of change in the position of flame front with time. The FSR increased in increase of wire diameter. The results show that flame front spreads sensitively to applied frequency and voltage in addition to wire diameter. Thus, further detailed analysis can be required, and presented in later section.

3.2 Flame spread rate

Figure 4 shows variations in FSR against f_{AC} at several voltages for (a) $D_{OUT} = 0.8$, (b) 1.1, and (c) 1.5 mm. The FSR, for the baseline case ($S_{W,0}$) with no applied electric field, was indicated with a black dot line.

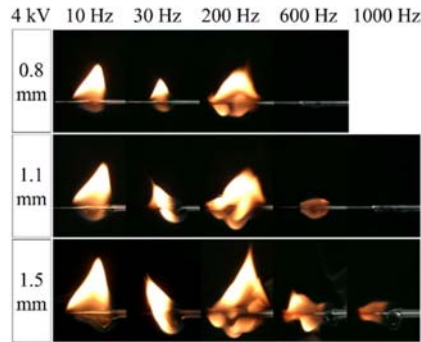


Figure 2 Instantaneous flame images with applied frequency for several wire diameters and frequencies at $V_{AC}=4$ kV

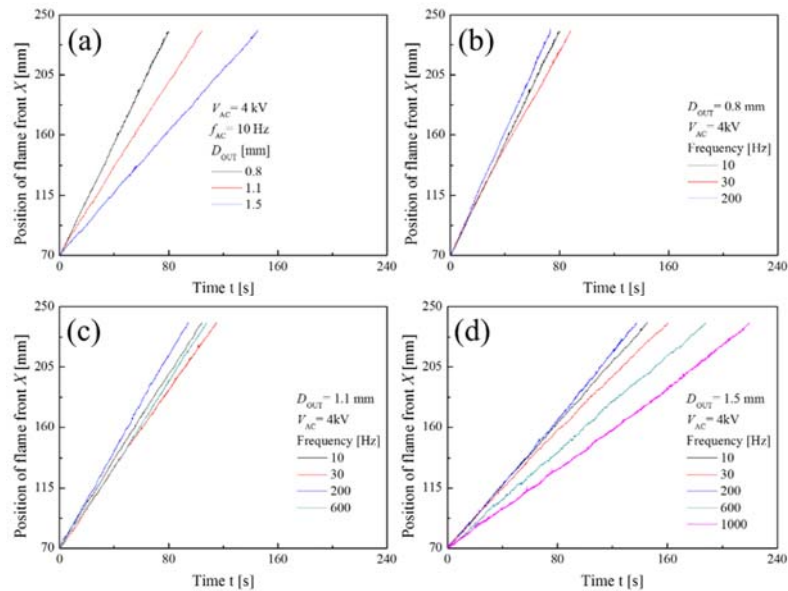


Figure 3 Temporal Position of flame front for (a) several diameters of wire at $V_{AC}=4$ kV, $f_{AC}=10$ Hz and various frequencies for (b) 0.8, (c) 1.1, (d) 1.5 mm in diameter

For $D_{OUT} = 0.8$ mm in Fig. 4(a), the FSR decreased in increase of f_{AC} at $V_{AC} = 1$ and 2 as well as at $f_{AC} \leq 200$ Hz for $V_{AC} = 3$ kV and at $f_{AC} \leq 80$ Hz for $V_{AC} = 4$ kV while the flame extinguished at $f_{AC} > 60$ Hz for $V_{AC} = 5$ kV. While, it increased again at $f_{AC} \geq 200$ Hz for $V_{AC} = 3$ kV, at $f_{AC} \geq 80$ Hz for $V_{AC} = 4$ kV. Note that all the FSRs with applied electric fields were smaller than that for the baseline case, except at $V_{AC} = 3$ kV and $f_{AC} = 1000$ Hz. For $D_{OUT} = 1.1$ and 1.5 mm in Figs. 4(b) and (c), the FSRs with applied electric fields decreased monotonously in increase of f_{AC} up to $V_{AC} = 3$ kV. However, when V_{AC} increased further for $D_{OUT} = 1.1$ and 1.5 mm, those decreased at $f_{AC} \leq 60$ (30) Hz and 4 (5) kV, increased at 60 (30) $\leq f_{AC} \leq 200$ (100) Hz for $V_{AC} = 4$ (5) kV, and then decreased again at $f_{AC} \geq 200$ (100) Hz for $V_{AC} = 4$ (5) kV, respectively. For $D_{OUT} = 1.1$ (0.8) mm, the flame extinguished at $f_{AC} > 600$ (200) Hz for $V_{AC} = 4$ kV and $f_{AC} > 400$ (60) Hz for $V_{AC} = 5$ kV. The flames did not extinguish in range of the current electric fields for $D_{OUT} = 1.5$ mm. Extinction limit was extended to higher frequency when the wire diameter increased. Considering the behaviors of the FSR with applied electric fields, it could be grouped into three distinct regimes depending on wire diameter as well as

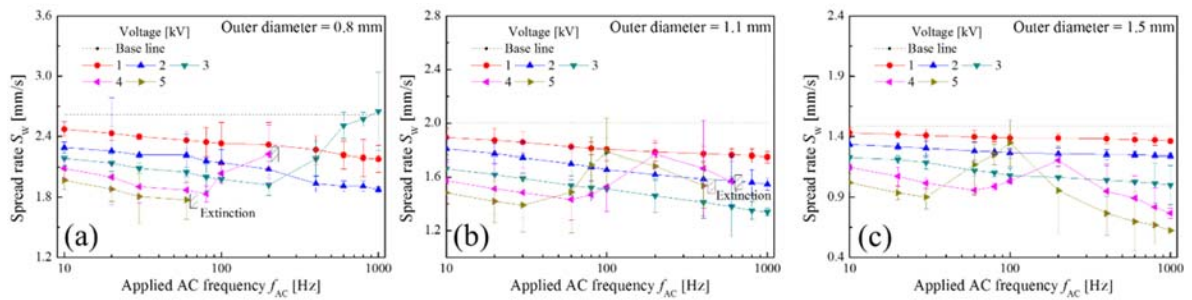


Figure 4 Flame spread rate against applied frequency at several voltages for (a) $D_{OUT} = 0.8$, (b) 1.1, and (c) 1.5 mm

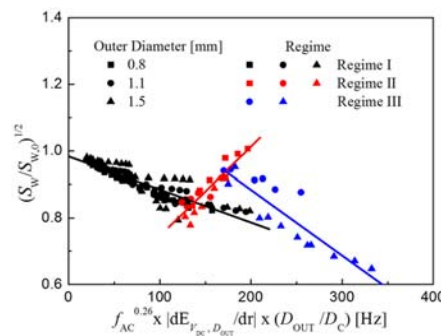


Figure 5 Characterization in flame spread rate for each regime.

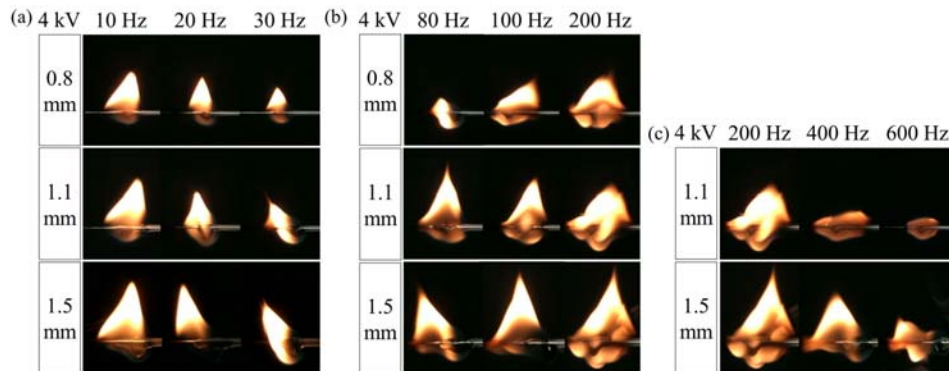


Figure 6 Representative flame images at (a) Regime I, (b) Regime II and (c) Regime III with applied electric fields and wire diameter

V_{AC} and f_{AC} : the FSR with V_{AC} and f_{AC} decreased monotonously in regime I, increased in regime II and then decreases again in regime III.

3.2 Characterization of flame spread rate

As mentioned above, the FSRs were influenced by wire diameter, applied V_{AC} and f_{AC} . Considering the relationship between the wire diameter and effect of electric field, variation in electric field intensity inside PE is important. The applied V_{AC} has a relationship with the rate of reduction of intensity electric field in

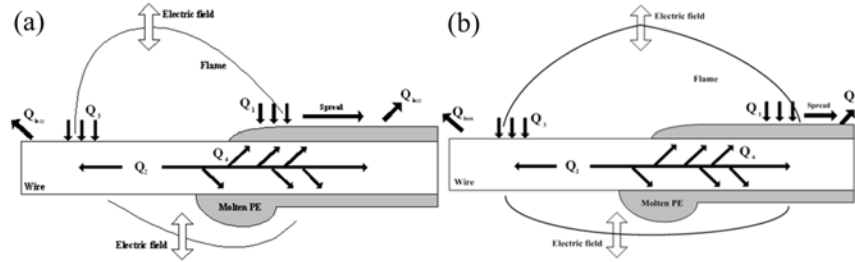


Figure 7 Schematic illustration of thermal balance mechanism in spreading flame.

PE depending on the wire diameter. Slope of intensity electric field, $dE_{V_{DC}, D_{OUT}}/dr$, was defined as the overall rate of change in the intensity electric field inside PE with radial direction. In characterization, V_{AC} could be replaced with an absolute values of $|dE_{V_{DC}, D_{OUT}}/dr|$. Intensities of electric field were calculated by using FEMM-4.2v for 0.8, 1.1 and 1.5 mm in diameter [9]. The FSRs could be characterized well by applied f_{AC} and absolute values of slope of intensity electric field as well as wire dimensionless in each regime.

$$C^* = f_{AC}^{0.26} \times \left| \frac{dE_{V_{DC}, D_{OUT}}}{dr} \right| \times \left(\frac{D_{OUT}}{D_C} \right) [Hz] \text{ and} \quad (1)$$

$$S^* = \left(\frac{S_W}{S_{W,0}} \right)^{\frac{1}{2}}. \quad (2)$$

Here, the absolute values of slope of intensity electric field inside PE was calculated by using FEMM-4.2v for 0.8, 1.1, and 1.5 mm in diameter [9]. Figure 5 shows that the behaviors of FSR are well characterized by C^* and S^* , i.e., $S^* = -0.00033C^* + 0.98$ (Correlation coefficient $R=0.89$) in regime I, $S^* = -0.00089C^* + 0.48$ ($R=0.90$) for regime II, and $S^* = -0.00066 C^* + 1.28$ ($R=0.90$) for regime III, respectively.

3.4 Thermal balance mechanism

Figure 6 exhibits the representative flame images with applied electric fields in regime I (a), regime II (b) and regime III (c). In regime I, the size of spreading flames became smaller in increase of V_{AC} and the flames were tilted to the bare wire in increase of V_{AC} and several diameters at a fixed f_{AC} as shown in Fig. 6(a). In regime II, the sizes of spreading flames were larger in increase of f_{AC} at a fixed V_{AC} as shown in Fig. 6(b). While, in regime III, the sizes were smaller again compared to those in regime II as shown in Fig. 6(c). Figure 7 illustrates the schematic representations of thermal balance mechanism for (a) regime I, III and (b) regime II. For the cases of regime I and III, the spreading flame The heat transfer from the flame to unburned PE (Q_1) is reduced in the situation of the leaning of flame to the bare wire. Moreover, as mentioned before, the flame size decreases appreciably with increasing V_{AC} and f_{AC} , this decreasing the heat transfer from the flame to the burnt wire (Q_3). Subsequently, the decrease in Q_3 causes reduction in the heat transfer to the molten PE through the wire (Q_2) and thereby to unburned wire (Q_4). Therefore, there will be reduction in the total heat transfer from the flame to PE, leading to the decrease of production and evaporation rate of molten PE. Consequently, the FSR becomes slower [7]. In the case of regime II case, The FSRs increases due to increasing increase in total heat transfer from the flame to PE with Q_1 and Q_3 .

4 Conclusions

An experimental study on flame spread over electrical wires with various insulator diameters under applied AC electric field was investigated in range of $V_{AC}=1-5$ kV and $f_{AC}=1-1000$ Hz. The results show that extinction limit (FSR) was extended (increased) in increase of wire diameter. The spreading flame was influenced significantly by wire diameter, applied V_{AC} and f_{AC} via changing the shape and size of flame. The FSRs having distinct three regimes, could be characterized by V_{AC} , f_{AC} and wire dimensions as well as absolute values of slope of intensity electric field inside PE. In each regime, the changing FSR could be explained by thermal balance mechanism.

5 Acknowledgements

This research was supported by SGER Program through the National Research Foundation of Korea (NRF) funded by the Ministry of Education.

References

- [1] Fujita O, Nishizawa K, Ito K. (2002). Effect of low External Flow on Flame Spread over Polyethylene-insulated Wire in Microgravity. Proc. Combust. Inst. 29:2545
- [2] Nakamura Y, Yoshimura N, Ito H, Azumaya K, Fujita O. (2009). Flame Spread over Electric Wire in Sub-atmospheric Pressure. Proc. Combust. Inst. 32:2559
- [3] Umemura A, Uchida M, Hirata T, Sato. (2002). Physical Model Analysis of Flame Spreading along an Electrical Wire in Microgravity. Proc. Combust. Inst. 29:2535
- [4] Onishi Y, Fujita O, Agata K, Takeuchi H, Nakamura Y, Ito H, Kikuchi M. (2010) Observation of Flame Spreading over Electric Wire under Reduced Gravity Condition Given by Parabolic Flight and Drop Tower Experiments. Transactions of the Japan society for Aeronautical and Space Sciences, Aerospace Technology Japan. Vol.8:19
- [5] Nakamura Y, Yoshimura N, Matsumura T, Ito H, Fujita O. (2008). Opposed-wind Effect on Flame Spread of Electric Wire in Sub-atmospheric Pressure. Journal of Thermal Science and Technology, Vol.3:430
- [6] Kikuchi M, Fujita O, Ito K, Sato A, Sakuraya T. (1998). Experimental study on flame spread over wire insulation in microgravity. Proc. 27th In. Comb. Symp.:2507
- [7] Kim MK, Chung SH, Fujita O. (2011). Effect of AC electric fields on flame spread over electrical wire. Proc. Combust. Inst. 33:1145
- [8] Lim SJ, Kim MK, Park J, Fujita O, Chung SH. (2104). Flame spread over electrical wire with AC electric fields: Internal circulation, fuel vapor-jet, spread rate acceleration, and molten insulator dripping. Combustion and Flame.
- [9] Finite Element Method Magnetics v-4.2.